Article:
Raiton, B, McLaughlan, JR, Harput, S et al. (3 more authors) (2012) The capture of flowing microbubbles with an ultrasonic tap using acoustic radiation force. Applied Physics Letters, 101 (4). 044102 - 044102. ISSN 0003-6951

https://doi.org/10.1063/1.4739514

The capture of flowing microbubbles with an ultrasonic trap using acoustic radiation force.

B. Raiton,[a] J. R. McLaughlan, S. Harput, P. R. Smith, D. M. J. Cowell, and S. Freear[b]
Ultrasound Group, School of Electronic and Electrical Engineering, University of Leeds, LS2 9JT, Leeds, UK.

(Dated: 13 July 2012)

The accumulation of 1-10 μm phospholipid-shelled microbubbles was demonstrated by creating an "ultrasonic tap" using acoustic travelling waves. Microbubbles were flowed through a 200 μm cellulose tube at rates ranging between 14-50 ml/hr, in order to approximate the velocities and wall shear rates found throughout the human circulatory system. The generated acoustic radiation force directly opposing the flow direction was sufficient to hold microbubbles in a fluid flow up to 28 cm/s. Clusters of microbubbles subject to wall shear rates of up to 9000 s^{-1} were retained near a pressure null for several seconds.

Due to renal clearance and enzymatic degradation, thrombolytic drugs have an insufficient half-life and high doses have to be administered to obtain satisfying therapeutic effects in the treatment of vascular diseases.[1] This leads to higher risks of hemorrhagic complications such as systemic bleeding. Encapsulation within liposomes or microbubbles (MB) lowers the protein immunogenecity and antigenicity, thus considerably extending the agent half-life. The drug can then be released at the target site upon insonication. Following intravenous injection, particle concentration drops significantly due to dilution throughout the blood volume.[2] Research is on-going to lower the systemic drug dose by improving the specificity of the delivery method toward the thrombus.[1] Attaching monoclonal antibodies such as antifibrin or antiplatelet onto the surface of MB slightly improves the efficacy of sonothrombolysis by increasing their concentration in the vicinity of the blood clot surface.[3] Targeting the thrombus in this way can also have beneficial effect on the safety of the delivery method by lowering the pressure threshold required to induce cavitation. Laing *et al.* reported that the targeting of liposomes to the disintegrating clot surface resulted in particles being displaced.[5] It has been shown that maximising the amount of cavitation events near the clot surface can significantly reduce the required systemic drug dose by facilitating its penetration into the thrombus.[6] Since stable cavitation can play an important role,[7] retaining the cavitation nuclei in the vicinity of the clot surface can further enhance the safety of the thrombolytic drug delivery. Non-invasively retaining MB onto the clot surface using low-intensity ultrasound traveling waves could benefit existing delivery techniques as it would apply to MB used as cavitation nuclei and drug-carriers.
The rheological behaviour of MB is similar to that of red blood cells which means they will generally flow along the centreline of microvessels.[8] Yet, for molecular recognition to occur, the microbubbles should be within 10-20 μm of the blood vessel lining or endothelium.[9] Acoustic radiation force can be used to "push" flowing MB towards the vessel walls to facilitate binding.[10] Rychak *et al.*[11] demonstrated a 44 fold increase in the number of bound MB through the use of radiation force, for a wall shear rate of 355 s^{-1} (centre frequency 2 MHz and peak negative pressure 122 kPa). However, there was still a drop of 75 % in the amount of bound MB, when the wall shear rate was increased to 1244 s^{-1}. Takalkar *et al.*[12] demonstrated that, once bound, MB can withstand wall shear rates of up to 16000 s^{-1} but the amount of MB retained was already down by 50% at 3400 s^{-1}.

In this letter we report on the creation of an acoustic radiation force tap to non-invasively trap and hold flowing MB at a single location. A null in the pressure field was created across a tube cross-section by emitting two ultrasound beams of opposite phase. The input beam duty factor was set to be lower than that of the output beam so that MB could enter the *low-pressure region*. Once trapped, MB were subject to a trapping force directly opposing the fluid flow. For wall shear rates of up to 9000 s^{-1}, MB aggregates were held within a *low-pressure region* (peak negative pressure < 350 kPa) for several seconds. An OEM diagnostic ultrasound probe was used to generate a pressure field with a centre frequency of 7 MHz, which is within the 1-10 MHz frequency range for ultrasound medical imaging.
Fig. 1 illustrates the use of the ultrasonic tap to accumulate and retain a MB population at the target site. The flowing MB formed aggregates as they first entered the ultrasound field. A translation towards the opposite tube wall then occurred near the peak of the input beam where the primary radiation force (PRF) is more significant. The Bjerknes principle predicts that MB excited above resonance are attracted to the pressure minima of an ultrasound field.[13] In the set-up shown in Fig. 1 a sufficient trapping force (TF) was generated to accumulate MB against the flow, within the *low-pressure region*. The excitation frequency was always set to 7 MHz, hence not all MB were affected by the trapping force.

[a] elbdr@leeds.ac.uk
[b] s.freear@leeds.ac.uk

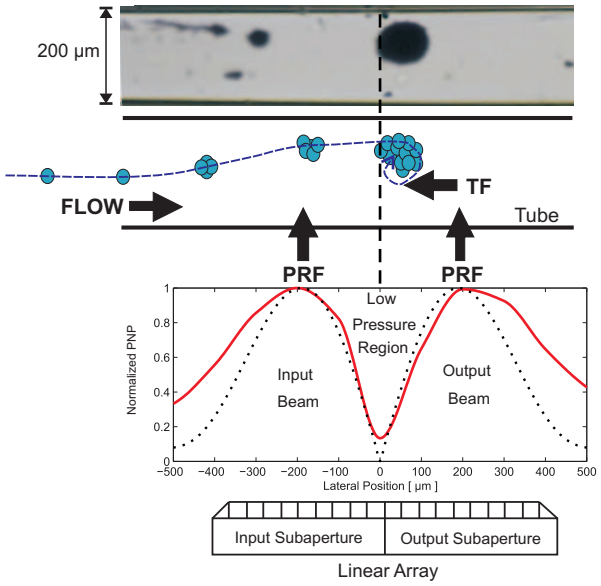

FIG. 1. (Top) A micrograph of the cellulose tube showing MB aggregation retained near the pressure null. (Middle) Schematic describing how the primary radiation force (PRF) causes MB aggregation and translation towards the opposite tube wall. The engendered trapping force (TF) directly opposes the flow direction thus trapping MB clusters. (Bottom) Simulated (dotted line) and measured (continuous line) lateral peak negative pressure (PNP) at the focal depth. The face of the linear array is parallel to the tube axis and the pressure null is aligned to its centre.

The generation of a pressure null through the interference of two acoustic waves of opposite phase was first verified experimentally. The 96-channel Ultrasound Array Research Platform[14] was used to drive a one-dimensional diagnostic ultrasound probe (L3-8/40EP, Prosonic, Korea). A 96-element aperture was focused at a depth of 30 mm. Two 48-element subapertures were configured to emit identical ultrasound pulses, with a phase shift of π. Fig. 1 shows a plot of the measured pressure field using a 200 μm needle hydrophone (Precision Acoustics Ltd., Dorchester, UK) mounted on a 3-D computer controlled translation system. The ultrasound probe and hydrophone were submerged within a tank of de-ionized and de-gassed water at 20±1°C. With the driving voltage set to its minimum and for a centre frequency of 7 MHz, the peak negative pressure (PNP) was measured to be 350 kPa for a lateral position of +200 μm and -200 μm. The width and slope gradient of the *low-pressure region* approximated the data simulated using the Field II package.[15,16]

Lipids were prepared by dissolving 1,2-Dipalmitoyl-snglycero-3-phosphocholine (DPPC), 1,2-Distearoyl-sn-glycero-3-phosphoethanolamine-N-[maleimide(polyethylene glycol)-2000] (DSPE-PEG2000), and 1,2-Dipalmitoyl-sn-glycero-3-phosphate (DPPA) from Avanti Polar Lipids (Alabaster, AL) in chloroform and drying them in a glass vial by a vacuum desiccator. Microbubbles were then obtained by resuspending the dried lipids in Dulbecco Phosphate-Buffered Saline (DPBS) with 1% glycerin by volume in a 1 mL vial. The solution was then saturated with C_3F_8 before being shaken for 45 seconds using a mechanical shaker. MB were then diluted in a cylindrical chamber that was immersed in de-gassed and de-ionized water at 20°C. The chamber was placed onto a mechanical stirrer to continuously mix its content during the experiment. A 1 mm hydrophone was located 10 mm from the chamber and at 90° in relation to a 5 MHz V310 transducer (Olympus-NDT Inc., Waltham, MA, USA) to acquire the scatter frequency spectrum from 3 to 8 MHz with 0.1 MHz steps. The average resonant frequency was measured to be 3.8 MHz. Micrographs of diluted MB were obtained using light microscopy and then analyzed using ImageJ (National Institute of Health, USA). The MB size distribution ranged from 1 to 10 μm with a mean diameter of 2 μm.

The MB were diluted to 40×10^6 MB/ml in de-gassed and de-ionised water then flowed through a 200 μm cellulose tube that was optically and acoustically transparent. The fluid flow rate was regulated with a programmable syringe pump (Aladdin-1000, World Precision Instruments, Sarasota, FL, USA), and an inverted microscope (Eclipse T*i*-U, Nikon, Melville, NY, USA) was used to optically image the tube. The ultrasound probe was aligned orthogonal to the tube and at a 45° angle in relation to the bottom of the tank.

When the "ultrasonic tap" was first applied, MB aggregated before the input beam and were unable to enter the *low-pressure region*. To remedy this, the ultrasonic tap was made to be asymmetrical by setting the input subaperture duty factor δ_i to be lower than that of the output subaperture, δ_o. To estimate what would be the best ratio $\alpha = \delta_i/\delta_o$, a concentration ($C_B$) of 1×10^9 MB/ml was flowed at a rate Q = 10 ml/hr. The output subaperture duty factor was set to 57 % with a pulse repetition frequency of 10 kHz and a PNP of 350 kPa. The experiment was repeated for α = 0.25, 0.5, 0.75 and 1. The most efficient accumulation was observed for a ratio $\alpha = 0.5$.

For the same ultrasound parameters, the performance of the ultrasonic tap was then evaluated at different flow rates with $C_B = 40\times10^6$ MB/ml. Image processing was performed in Matlab (Mathworks Inc., Natick, MA, USA) on the recorded videos to track the diameter and position of the largest cluster. The cluster accumulation duration t_{acc} and the maximum diameter d_{max} it reached are listed in table I for each value of Q. The cluster resting position before it exit the trap was always between 70 and 110 μm from the pressure null. For a flow rate of 40 ml/hr a 9.5 μm cluster was retained 70 μm away from the pressure null for 1.4 s.

The syringe driver was then set to its maximum flow rate of 50 ml/hr and the output duty factor was

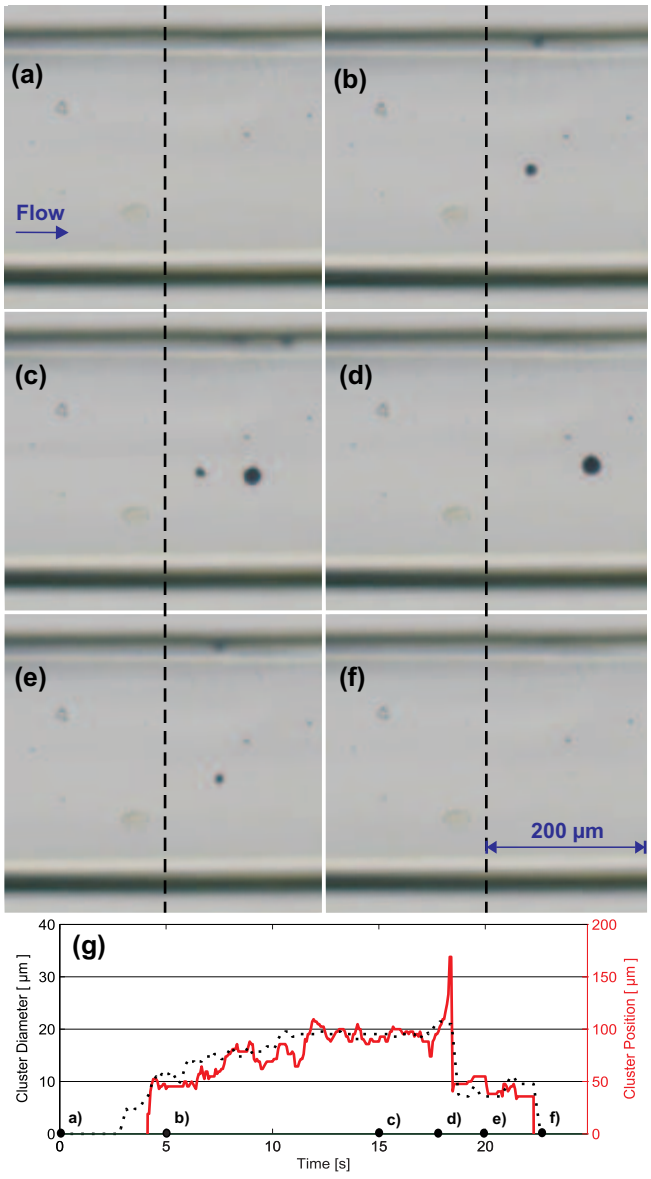

FIG. 2. In the series of micrographs (a)-(f) the flow rate and concentration were 50 ml/hr and 40×10^6 MB/ml respectively. The vertical dotted lines at the centre of each micrograph represent the pressure null. (g) is a plot of the largest trapped cluster diameter (dotted line) and position (continuous line). The centre frequency was 7 MHz, the pulse repetition frequency 10 kHz, the PNP of 500 kPa, $\delta_s = 71\%$ and $\alpha = 0.5$.

increased to 71 %. The ratio between input and output duty factor was kept at 0.5. For a PNP of 350 kPa, a 12 μm cluster was retained 95 μm beyond the pressure null for 1.6 s. The cluster diameter then became too great for the trapping force to retain it. To intensify the trapping force, the PNP was raised to 500 kPa. Fig. 2(a)-(f) is a series of micrographs acquired at different times during the experiment. The tracking of the cluster diameter and position are plotted in Fig. 2(g). Before the ultrasound source was activated (Fig. 2(a)) only imperfections were visible between the tube walls. Although MB were flowing past the region imaged, they were not visible due to the high flow rate. It took 3 s for a first cluster to enter the *low-pressure region* (Fig. 2(g)). In Fig. 2(b) it had reached a diameter of 11.4 μm and continued to accumulate MB for a further 5 s. As it then stopped accumulating MB, its diameter and position remained around 19 μm and 90 μm for 7 s. In Fig. 2(d) the cluster size increased beyond 20 μm and, as the trapping force wasn't sufficient, it started to shift away. It was replaced by a smaller 7 μm cluster that remained held (Fig. 2(e)) until the end of the ultrasound exposure (Fig. 2(f)).

TABLE I. Maximum cluster diameter d_{max} and accumulation duration t_{acc} for an increasing flow rate Q. The ultrasound parameters were constant with a centre frequency of 7 MHz, a pulse repetition frequency of 10 kHz, a PNP of 350 kPa, $\delta_s = 57\%$ and $\alpha = 0.5$. The MB concentration was 40×10^6 MB/ml.

Q (ml/hr)	14	16	20	30	40
d_{max} (μm)	32	22	19	11.9	9.5
t_{acc} (s)	13	5.3	4.5	2.7	1.4

In Newtonian flow the wall shear rate is $\gamma_w = 32Q/\pi D^3$ and the corresponding mean velocity is $v_z = D\gamma_w/8$. The tube internal diameter D was observed to expand to 250 μm when filled with water. Thus, a flow rate of 50 ml/hr was expected to induce mean velocities nearing 28 cm/s and wall shear rates of up to 9000 s^{-1}. Applying radiation force orthogonal to the flow in large arteries to stop flowing MB remains a challenge as mean velocities can reach several cm/s. Patil *et al.*[17] reported that, even when excited near resonance, a mechanical index of 0.15 was required to halt MB for a wall shear rate of 52 s^{-1}. Moreover, flowing MB clusters can impede accumulation by engulfing already bound targeted MB.[9] Through the generation of a trapping force directly opposing the flow, the ultrasonic tap was able to halt MB subject to wall shear rates of up to 9000 s^{-1}. Yet the mechanical index of the pressure field at the focal depth was 0.13. The diameter of the tube used in the experiments was similar to that of capillaries. However, for the same mean velocity, the MB accumulation is expected to be more significant in larger vessels such as arteries due to the lower wall shear rates. Fig. 2 demonstrates that, instead of attracting trapped MB as they flow past, clusters would accumulate at the target site.

Maxwell *et al.*[18] recently reported on the ability to use standard imagine techniques such as power doppler and B-mode imaging to guide and monitor clot fragmentation in porcine models. The same principle could be applied with the ultrasonic tap to align MB clusters to the clot surface. Shifting the input and output subapertures across the array elements would laterally translate the pressure null along the thrombus without having to

move the transducer itself. There is a clear advantage in using a single ultrasound transducer not only to image the target region but also induce stable cavitation to enhance clot permeation and inertial cavitation to released encapsulated drugs.[1] In this preliminary study it was demonstrated that a standard linear array could be used to induce a *low-pressure region* capable of retaining MB subject to wall shear rates of up to 9000 s^{-1}.

B.R. would like to thank the Royal Academy of Engineering and Elster Instromet for their financial support. This work was supported by ESPRC grant number EP/I000623/1.

[1] B. Vaidya, G. P. Agrawal, and S. P. Vyas, Int. J. Pharm. **424**, 1 (2012)
[2] L. E. Deelman, A. Decleves, J. J. Rychak, and K. Sharma, Adv. Drug Deliver. Rev. **62**, 1369 (2010)
[3] F. Xie, J. Lof, T. Matsunaga, R. Zutshi, and T. R. Porter, Circulation **119**, 1378 (2009)
[4] S. T. Ren, H. Zhang, Y. W. Wang, B. B. Jing, Y. X. Li, Y. R. Liao, X. N. Kang, W. J. Zang, and B. Wang, Ultrasound Med. Biol. **37**, 1828 (2011)
[5] S. T. Laing, M. R. Moody, H. Kim, B. Smulevitz, S.-L. Huang, C. K. Holland, D. D. McPherson, and M. E. Klegerman, Thrombosis Research (2011)
[6] S. Datta, C. Coussios, A. Y. Ammi, T. D. Mast, G. M. de Courten-Myers, and C. K. Holland, Ultrasound Med. Biol. **34**, 1421 (2008)
[7] S. Datta, C. C. Coussios, L. E. McAdory, J. Tan, T. Porter, G. D. Courten-Myers, and C. K. Holland, Ultrasound Med. Biol. **32**, 1257 (2006)
[8] J. R. Lindner, J. Song, A. R. Jayaweera, J. Sklenar, and S. Kaul, J. Am. Soc. Echocardiog. **15**, 396 (2002)
[9] B. J. Schmidt, I. Sousa, A. A. van Beek, and M. R. Bohmer, J. Control. Release **131**, 19 (2008)
[10] P. A. Dayton, J. S. Allen, and K. W. Ferrara, J. Acoust. Soc. Am. **112**, 2183 (2002)
[11] J. Rychak, A. Klibanov, and J. Hossack, IEEE Trans. Ultrason. Ferroelectr. Freq. Control. **52**, 421 (2005)
[12] A. M. Takalkar, A. L. Klibanov, J. J. Rychak, J. R. Lindner, and K. Ley, Journal of Controlled Release **96**, 473 (2004)
[13] T. G. Leighton, A. J. Walton, and M. J. W. Pickworth, Eur. J. Phys. **11**, 47 (1990)
[14] P. R. Smith, D. M. J. Cowell, B. Raiton, C. V. Ky, and S. Freear, IEEE Trans. Ultrason. Ferroelectr. Freq. Control. **59**, 40 (2012)
[15] J. Jensen and N. Svendsen, IEEE Trans. Ultrason. Ferroelectr. Freq. Control. **39**, 262 (1992)
[16] J. A. Jensen, in *10th Nordic-Baltic Conference on Biomedical Imaging Published in Medical & Biological Engineering & Computing* (1996) pp. 351–353
[17] A. V. Patil, J. J. Rychak, J. S. Allen, A. L. Klibanov, and J. A. Hossack, Ultrasound Med. Biol. **35**, 2021 (2009)
[18] A. D. Maxwell, G. Owens, H. S. Gurm, K. Ives, D. D. M. Jr, and Z. Xu, Journal of Vascular and Interventional Radiology **22**, 369 (2011)